Sensors and Materials, Vol. 12, No. 5 (2000) 315–325
MYU Tokyo

S & M 0412

YBaCuO Uncooled Microbolometer IRFPA

Hideo Wada, Takanori Sone,[1] Hisatoshi Hata,[1]
Yoshiyuki Nakaki,[1] Osamu Kaneda,[1] Yasuaki Ohta,[1]
Masashi Ueno[1] and Masafumi Kimata[1]

Technical Research and Development Institute Japan Defense Agency
1-2-24, Ikejiri, Setagaya-ku, Tokyo 154-8511, Japan
[1]Advanced Technology R & D Center, Mitsubishi Electric Corporation
4-1, Mizuhara, Itami, Hyogo 664-8641, Japan

(Received July 3, 2000; accepted September 19, 2000)

Key words: YBaCuO film, microbolometer, uncooled infrared focal plane, thermal imaging

An uncooled microbolometer focal plane array (FPA) using semiconducting YBaCuO films has been developed. Because the semiconducting YBaCuO films have a temperature coefficient of resistance (TCR) of over 3%/K at room temperature, they are considered to be candidates for bolometer materials of uncooled infrared (IR) detectors. There is a problem, however, in that the resistivity of the films is over 10 Ωcm, which is two orders of magnitude higher than that of conventional VO_x bolometer films. To decrease the resistance of the bolometers, we combined them with comb-shaped electrodes. When the YBaCuO film was deposited on these electrodes by RF magnetron sputtering at ambient temperature in an atmosphere of 2% O_2 and 98% Ar, it showed a resistivity of 90 Ωcm and a TCR of –3.2%/K; ultimately the bolometer resistance became 82 kΩ using the comb-shaped electrodes. The YBaCuO bolometer detector which we have developed contains an infrared absorbing membrane with a high fill factor of 90% to achieve high infrared absorption. In a vacuum, the detector showed a thermal conductance of 1.3×10^{-7} W/K and a responsivity of 5.9×10^5 V/W. The fabricated FPA has an array format of 320 × 240 pixels and a pixel pitch of 40 μm. Finally, the FPA was integrated into a vacuum package and set on the focal plane of a prototype camera to obtain IR images. The YBaCuO microbolometer FPA showed a noise equivalent temperature difference (NETD) of 0.08 K with f/1.0 optics.

1. Introduction

In the past several years, uncooled infrared focal plane arrays (IRFPAs) have been enthusiastically studied to reduce the cost, size and weight of infrared cameras. In particular, exciting progress has been made in VO_x microbolometer FPAs, which have become commercially available products.[1,2] However, higher performance of uncooled FPAs is required for a wide range of military and commercial IR imaging applications.

Methods for enhancing the sensitivity of microbolometer FPAs mainly improve the thermal isolation of detectors (that is, to decrease their thermal conductance) and increase the temperature coefficient of resistance (TCR) of bolometer materials. Regarding thermal conductance, a recent study achieved a value of less than 0.3×10^{-7} W/K, which is within one-tenth of the theoretical limit.[3] Significant decrease in the thermal conductance will be difficult because the thermal capacity of the thermally isolated detectors must also be reduced. Otherwise, the thermal time constant of the detectors will increase over the permissible values. In terms of TCR, conventional VO_x bolometers show a value of approximately 2%/K at room temperature, and amorphous silicon (a-Si), which has recently been studied as a bolometer material, shows a TCR of approximately 2.5%/K, which slightly exceeds that of VO_x. However, the a-Si bolometers exhibit larger 1/f noise than VO_x; therefore, the reason for an a-Si bolometer FPA is not higher performance but low cost resulting from the advantage of full compatibility with Si-CMOS technology.[4]

Semiconducting YBaCuO thin films have high TCRs, and hence they are considered candidates for IR bolometer materials.[5,6] The TCR is over 3%/K at room temperature, but the resistivity is over 10 Ωcm, which is much higher than that of VO_x. For highly resistive bolometers, we cannot simply adopt conventional readout circuits.

To decrease the resistance of the YBaCuO bolometers, we combined the bolometers with comb-shaped electrodes. The resistance of the bolometers was less than 100 kΩ, which is almost comparable with VO_x bolometers. Therefore, we can adopt a conventional readout circuit for the YBaCuO bolometers using comb-shaped electrodes. By using both standard LSI and post-LSI process lines, we have developed a 320×240 pixel FPA with the YBaCuO microbolometers. The detectors on the FPA also contain an IR absorbing membrane with a high fill factor to achieve high IR absorption.[7]

In this paper, we describe the detector structure, its fabrication and the readout circuit of the FPA. We also report the properties of the YBaCuO bolometers and the detectors of the fabricated FPA. We then integrate the FPA into a vacuum package and report its performance when operated with a prototype infrared camera.

2. Materials and Methods

2.1 *Fabrication*[7]

The fabrication of YBaCuO microbolometer detectors is divided into a standard LSI process and a post-LSI process. A post-LSI process is necessary to perform YBaCuO film deposition and subsequent steps, because the YBaCuO film materials are incompatible with the silicon-LSI process.

Figure 1 shows the flow of the fabrication process for the YBaCuO microbolometer detectors. First, amorphous Si is deposited as a sacrificial layer using RF magnetron

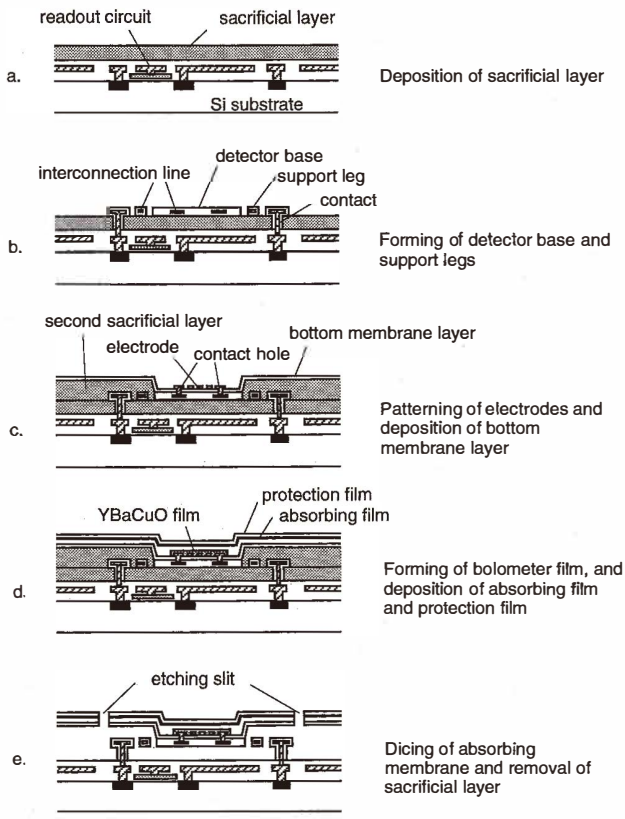

Fig. 1. Process flow for the YBaCuO microbolometer detector.

sputtering on the top of the Si substrate including CMOS readout circuits as shown in Fig. 1(a). In the following step shown in Fig. 1(b), the sacrificial layer is selectively etched to make contacts between the CMOS circuit and the detectors. The detector base and its support legs are formed from a two-layered structure with CVD-SiO_2 and CVD-SiN films, which are deposited on the sacrificial layer. This two-layered structure has an interconnection line between the SiO_2 and SiN films.

A second sacrificial Si layer is deposited and patterned by removing it in the area of the detector base. A CVD-SiO_2 film, which constitutes the bottom membrane of an IR absorbing structure, is deposited on the second sacrificial layer. Next, contact holes are formed on the detector base to make contacts between the interconnection lines and electrodes. A platinum (Pt) film for the electrodes is deposited on the bottom membrane and patterned into a comb-shape by dry-etching as shown in Fig. 1(c).

The YBaCuO bolometer film is deposited on the electrodes by RF magnetron sputtering. The sputtering is carried out with a $YBa_2Cu_3O_{6+x}$ target under Ar and O_2 atmospheres

at a chamber pressure of 1.3 mTorr. The bolometer film is protected by a CVD-SiN film; then, a metallic film with a sheet resistance of 377 Ω/ and a CVD-SiN film are successively formed on the protective film as shown in Fig. 1(d). This metallic film functions as an IR absorbing film on a cavity absorbing structure which is constructed from the metallic film, a conduction layer of the readout circuit, and an optical gap between the metallic film and the conduction layer. The outermost SiN film functions as the top membrane of the absorbing structure as well as the protecting film of the detector. Next, this absorbing membrane is diced with etching slits to separate each pixel. The area of this patterned membrane equals the IR absorbing area of the detector. Finally, two sacrificial layers are removed by etching to achieve a thermally isolated structure as shown in Fig. 1(e).

2.2 *Readout circuit design of FPA*

A block diagram of the readout circuit of the FPA is shown in Fig. 2. Sample-hold circuits composed of a sampling switch (S_i) and a sampling hold capacitor (C_i) are arranged at the end of each column, while at the beginning of each column constant current sources (M_i) are arranged so that a constant current flows into the bolometers (R_{ij}). The suffixes i and j indicate the numbers of the columns and the rows of the array,

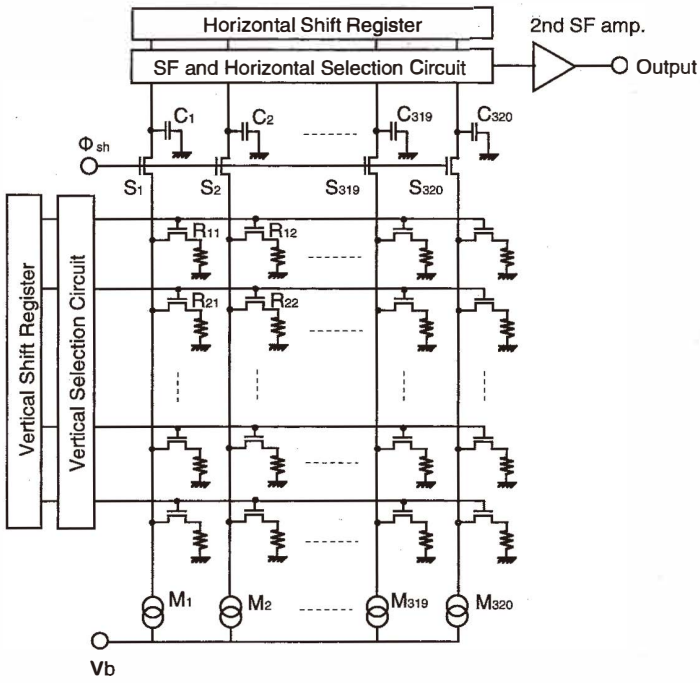

Fig. 2. Readout circuit diagram of FPA.

respectively. When horizontal lines are selected by the vertical selection circuit, each vertical line generates a signal voltage from the bolometers applied with a bias voltage V_b. The signal voltage depends on the resistance of the bolometer; this voltage is lower when the irradiated IR power is higher, because the bolometer resistance decreases when its temperature rises as the intensity of the infrared radiation increases. When the sampling switch is closed by the clock pulse ϕ_{sh}, the signal voltage is stored in the sample hold capacitor. The stored signal is successively read out by the horizontal select circuit through source followers (*SF*).

Because of the sample-hold circuits, the biased time of the bolometers may be extended up to the full readout time of the horizontal line; therefore, it is possible to allow only a single output terminal for the readout circuit of the FPA.

2.3 *Measurements*

Preliminary electrical measurements with the YBaCuO bolometer films were performed for resistance, TCR and noise. For these measurements, we selected detectors of a test element group (TEG) which were fabricated simultaneously with the FPA. The sacrificial Si layers of these detectors were left in place, to avoid temperature increase of the detector during the electrical measurements. The terminal pads of the TEG which directly led to the bolometer electrodes via conduction lines were connected to the measurement apparatus.

To measure properties of the detector such as thermal conductance and thermal capacity, the sacrificial layers of the detectors were removed. The TEG chips were built into a vacuum chamber and connected to the outer apparatus. Thermal conductance was given by the measurement of the temperature increase depending on the biased power. The thermal capacity was given by the measurement of the time constant of the detector which was estimated from its temperature change when the instantaneous change in the bias voltage was produced.

To measure the performance of the FPA, the FPA chip in turn was built into a vacuum chamber and electrically connected into a prototype camera circuit. Figure 3 shows the setting for the measurement of responsivity. The chamber has an 8~12 μm infrared window to enable the FPA to be exposed to external IR radiation. The IR radiation originates from a calibrated blackbody and passes through optical slits. The responsivity is derived from the signal voltage of the camera, which depends on the irradiated IR power.

Finally, the fabricated FPA was integrated into a vacuum package and set in the prototype camera. The NETD of the FPA was measured using the camera and the blackbody.

3. Results and Discussion

3.1 *Properties of YBaCuO bolometer films*

Figure 4 shows the resistivity of the YBaCuO films as a function of the O_2 content of the sputtering atmosphere. The resistivity is minimized in an atmosphere of 2% O_2 and is 90 Ωcm at room temperature. We adopted a pair of comb-shaped electrodes for the

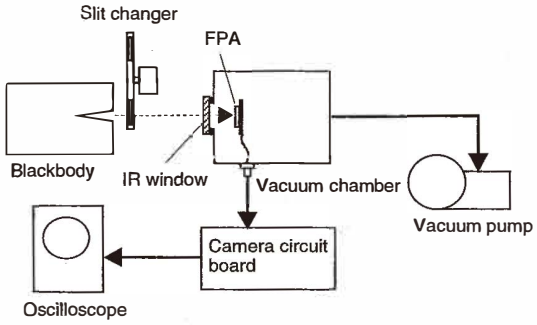

Fig. 3. Experimental set-up for response measurement.

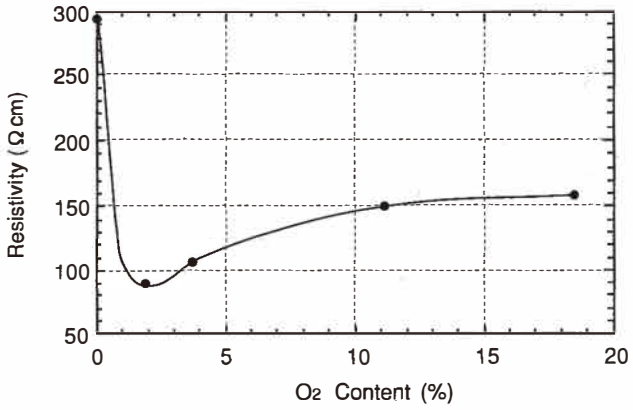

Fig. 4. O_2-dependence of YBaCuO film resistivity.

detectors, one with two teeth and the other with three. The width of the teeth is 1.5 μm and their length is 12.5 μm. The electrodes are placed so that the gap between them is 1.5 μm at every point. When the 3500-Å-thick YBaCuO film is fabricated on the comb-shaped electrodes under 2% O_2 sputtering atmosphere, the bolometer resistance is 82 kΩ at 300 K. Figure 5 shows the temperature change of the resistance under these conditions. The slope of ln$R$ vs $1/T$, where R is resistance and T is temperature, is almost constant from 300 K to 333 K. Hence, the constant B derived from the equation $R = R_0\exp(B/T)$ equals 2835 K. Since the TCR is derived from the expression $-B/T^2$, the TCR at 300 K is –3.2%/K, which is larger than the –2.0%/K of the typically reported value of VO_x.

Figure 6 shows the voltage noise spectral density Sv of the YBaCuO film measured at room temperature with a bias voltage of 3.5 V (or a bias current of 44 μA). The peaks at 40 Hz and 60 Hz correspond to environmental pickup by the measuring apparatus. We observed 1/f noise in the low-frequency region: for example, $\sqrt{Sv}$~500 nV/$\sqrt{\text{Hz}}$ at 10

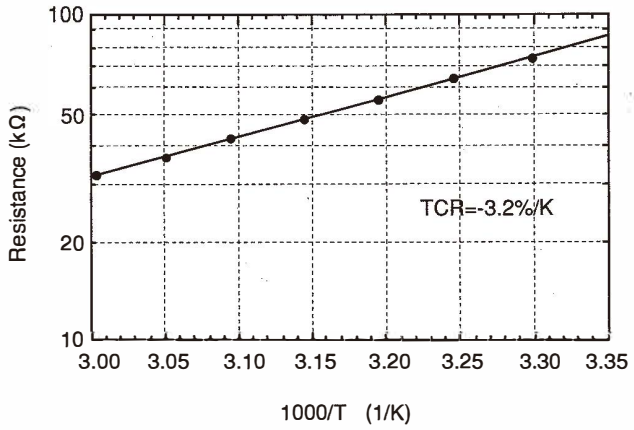

Fig. 5. Temperature dependence of bolometer resistance.

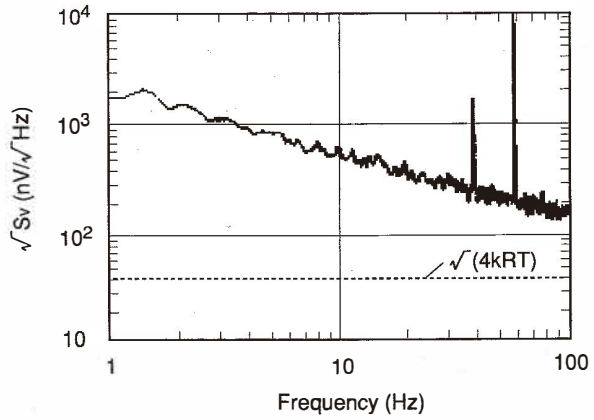

Fig. 6. Voltage noise spectrum of YBaCuO bolometer film; the dotted line shows the theoretical Johnson noise.

Hz against the theoretical Johnson noise of 40 nV/$\sqrt{}$ Hz. When this 1/f noise is estimated by a quantitative comparison under conditions of a constant operating power, the YBaCuO bolometer shows the same level as VO_x bolometers.[6,8] The total rms noise of the bolometer within 200 kHz is 21 μVrms; therefore, the YBaCuO film is an excellent low noise resistor for microbolometers.

3.2 *Properties of YBaCuO bolometer detector*

Figure 7 shows the SEM micrograph of a finished bolometer array. The bolometer film is patterned within the center squares which appear as if they are drawn with white

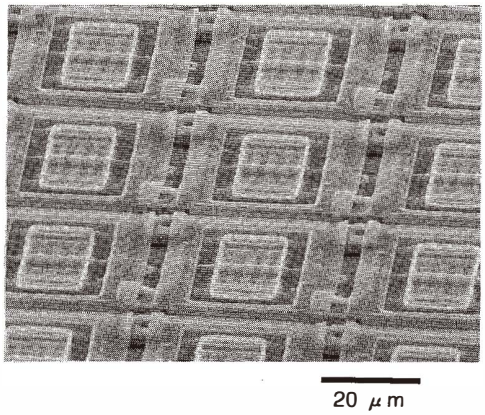

Fig. 7. SEM micrograph of microbolometer array.

outlines. The comb-shaped electrodes are faintly visible underneath the bolometer. The area of the square which immediately surrounds the bolometer square is identical to the detector base. The square outside the detector base is the IR absorbing membrane, the periphery of which covers the support legs. The fill factor of the pixel is 90% with the IR absorbing membrane. The support legs are L-shaped with a total length of 49 μm and a width of 1.5 μm. The thermal conductance of the detector achieves a value of 1.3×10^{-7} W/K with the support legs. It is considered that the IR absorbing ability is mainly due to the area of the absorbing membrane except on the electrodes, because the metal of the electrodes has a high IR reflectance. The main absorbing area is divided into two areas: the detector base, except on the bolometer, and the periphery of the absorbing membrane. The results of the measurement of IR absorptance of these areas were derived from a method of optical thin film calculations and are shown in Fig. 8. In this calculation, we assumed that the air gaps in the detector base and the periphery of the absorbing membrane equal the thickness of these sacrificial layers; that is, 0.8 μm for the detector base and 1.6 μm for the periphery of the absorbing membrane. The cavity absorbing structures of the two areas are almost optimized by the presence of the insulating films under the IR absorbing film, even if the air gaps are 0.8 μm and 1.6 μm, respectively. Consequently, the absorbing areas show a high average absorptance of over 80% between 8 and 12 μm as shown in Fig. 8.

3.3 *Performance of YBaCuO Microbolometer FPA*

To measure the responsivity of the detector, the 320×240 pixel microbolometer FPA was set in the vacuum chamber and electrically connected to the camera circuit. The bolometer of the FPA was fabricated under the conditions already mentioned. The FPA was operated at a TV standard frame rate with 15.73 kHz vertical scanning rate and 6.1 MHz horizontal scanning rate. The bias current of the bolometer in each pixel was controlled at about 40 μA, and the mean output voltage was 4 V in the circuit.

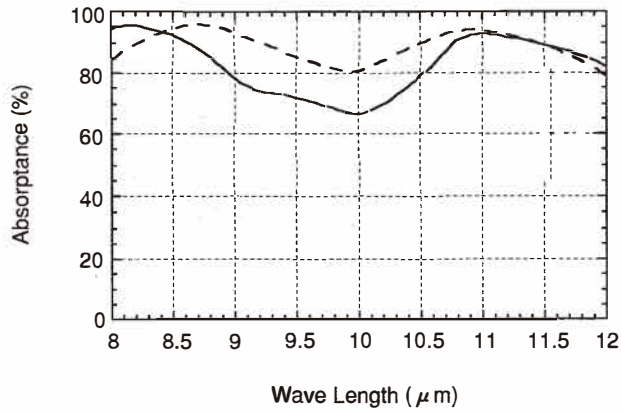

Fig. 8. Absorptance of detector: detector base excluding electrodes (solid curve) and periphery of absorbing membrane (dashed curve).

The voltage responsivity was 5.9×10^5 V/W when the IR power was irradiated from the black body at 323 K. The responsivity Rv is expressed by the equation

$$Rv = \frac{\varepsilon \alpha V}{G}, \text{ (V/W)} \tag{1}$$

where ε is the effective IR absorptance of the detector, α is the TCR, V is the bias voltage and G is the thermal conductance. We may estimate an effective IR absorptance of 69% from the measured values. It can be considered that the absorptance lower than the detector base excluding the electrodes (~80%) or the periphery of the absorbing membrane (~85%) which is shown in Fig. 8 result from the area of the bolometer electrodes.

Finally, the microbolometer FPA was integrated into the vacuum package and placed at the focal plane of the IR camera. This camera includes an f/1.0 optical lens and correction circuits for nonuniformity in bolometer resistance and responsivity. The FPA was operated under the conditions mentioned above. An example of the resulting images is shown in Fig. 9, for which the NETD of the FPA was 0.08 K.

The main properties of the YBaCuO microbolometer FPA are summarized in Table 1.

4. Conclusions

We have developed an uncooled IRFPA with YBaCuO microbolometers. The YBaCuO microbolometer films were deposited by RF magnetron sputtering at ambient temperature in an atmosphere of 2% O_2 and 98% Ar. The YBaCuO films developed showed a TCR of

Fig. 9. Infrared image obtained from 320×240 YBaCuO microbolometer FPA.

Table 1
Summary of YBaCuO microbolometer FPA.

Detecting method	YBaCuO Bolometer
Number of pixels	320 [H] × 240 [V]
Pixel size	40 μm × 40 μm
Fill factor	90%
Thermal conductance	1.3×10^{-7} W/K
Heat capacity	2.2×10^{-9} J/K
TCR	–3.2%/K
IR absorption (estimation)	69%
Responsivity	5.9×10^{5} V/W
NETD (f/1.0)	0.08 K

–3.2%/K and a resistivity of 90 Ωcm. To decrease the resistance of the bolometers, the bolometer films were combined with comb-shaped electrodes resulting in a resistance of 82 kΩ at 300 K. The YBaCuO bolometer detector, which includes an infrared absorbing membrane, is characterized by a fill factor of 90% and an infrared absorption of 69%. The readout circuit of the FPA includes sample-hold circuits in each column, which make possible a single outlet. The 320 × 240 pixel FPA operated with a prototype camera showed a responsivity of 5.9×10^5 V/W and an NETD of 0.08K with f/1.0 optics in a vacuum.

Acknowledgment

The authors thank T. Seto and N. Ohkawa from Kamakura Works of Mitsubishi Electric for their support of the measurements using the prototype camera.

References

1 B. Meyer, R. Cannata, A. Stout, A. Gin, P. Taylor, E. Woodbury, J. Deffner and F. Ennerson: SPIE **2746** (1996) 13.
2 T. Breen, N. Butler, M. Kohin, C. A. Marshall, R. Murphy, T. Parker and R. Silva: SPIE **3379** (1998) 145.
3 W. Radford, D. Murphy, A. Finch, K. Hay, A. Kennedy, M. Ray, A. Sayed, J. Wyles, R. Wyles, J. Varesi, E. Moody and F. Cheung: SPIE **3698** (1999) 119.
4 J. L. Tissot, F. Rothan, C. Vedel, M. Vilain and J. J. Yon: SPIE **3379** (1998) 139.
5 P. C. Shan, Çelik-Butler, D. P. Butler and A. Jahanzeb: J. Appl. Phys. **78** (1995) 7334.
6 A. Jahanzeb, C. M. Travers, Z. Çelik-Butler, D. P. Butler and S. G. Tan: IEEE Trans. Electron Devices **44** (1997) 1795.
7 T. Ishikawa, M. Ueno, K. Endo, Y. Nakaki, H. Hata, T. Sone and M. Kimata: Opto-Electr. Rev. **7** (1999) 297.
8 C. Marshall, N. Butler, R. Blackwell, R. Murphy and T. Breen: SPIE **2746** (1996) 23.